Reaching Fractional Quantum Hall States with Optical Flux Lattices

Nigel R. Cooper[1] and Jean Dalibard[2,3]

[1]*T.C.M. Group, Cavendish Laboratory, J. J. Thomson Avenue, Cambridge CB3 0HE, United Kingdom*
[2]*Laboratoire Kastler Brossel, CNRS, UPMC, ENS, 24 rue Lhomond, F-75005 Paris, France*
[3]*Collège de France, 11, place Marcelin Berthelot, 75005 Paris, France*

(Received 14 December 2012; published 29 April 2013)

We present a robust scheme by which fractional quantum Hall states of bosons can be achieved for ultracold atomic gases. We describe a new form of optical flux lattice, suitable for commonly used atomic species with ground state angular momentum $J_g = 1$, for which the lowest energy band is topological and nearly dispersionless. Through exact diagonalization studies, we show that, even for moderate interactions, the many-body ground states consist of bosonic fractional quantum Hall states, including the Laughlin state and the Moore-Read (Pfaffian) state. These phases are shown to have energy gaps that are larger than temperature scales achievable in ultracold gases.

DOI: 10.1103/PhysRevLett.110.185301 PACS numbers: 67.85.−d, 37.10.Vz, 73.43.−f

There is intense interest in finding new settings in which topological phases of matter analogous to fractional quantum Hall (FQH) states appear. Ultracold atomic gases are ideal systems with which to achieve this goal: they allow studies of strong correlation phenomena for both fermions and bosons, and FQH physics can be approached for homogeneous fluids [1] as well as for atoms confined in optical lattices [2].

While existing theories of FQH-like phases in lattices have focussed on tight-binding models [3–12], one of the most promising routes to topological flat bands for ultracold atoms is through optical flux lattices (OFLs) [13–15]. An OFL uses a set of laser beams to produce a spatially periodic atom-laser coupling that induces resonant transitions between two (or more) internal atomic states. The resulting energy bands, in particular the lowest one, have nonzero Chern numbers, and can be made narrow in energy [15]. This opens the path to experimental studies of novel strong correlation phenomena in topological flat bands, notably the FQH effect of bosons.

We present, in this Letter, the first characterization of the many-body ground state of bosons in an OFL. We start with the design of a novel type of OFL, which fully exploits the structure of the most commonly used (bosonic) atomic species. We devise a method to optically dress three internal states in a more general manner than previous OFL proposals [13,14], which leads to much narrower topological bands [15]. Our proposed OFL scheme is highly robust: it uses three coplanar optical beams derived from a single laser source, which do not require relative phase locking. For optimized parameters the lowest band of the OFL has Chern number 1 and is nearly dispersionless, closely analogous to the lowest Landau level for a charged particle in a uniform magnetic field. We use exact diagonalization to determine the many-body spectrum of a bosonic gas in this OFL. We show that FQH ground states appear for relatively weak atom interaction at the same filling factors as for a continuum Landau level [1]. Our work provides a concrete experimental scheme by which FQH states of bosons can be realized with large energy scales. Furthermore, it provides the first example of a non-Abelian quantum Hall state (the $\nu = 1$ Moore-Read state [16]) in a lattice model at high particle density with only two-body interactions.

We focus, in this Letter, on the case of atoms with ground state angular momentum $J_g = 1$, which is the case for several bosonic isotopes of alkali metal species. We denote $|X\rangle$, $|Y\rangle$, $|Z\rangle$ a basis of the ground state, defined such that $\hat{J}_X|X\rangle = 0$ (and similarly for Y and Z). Here the set of directions X, Y, Z represents an orthogonal trihedron of the physical space [see Fig. 1(a)] and $\hat{J}_X$ stands for the component of the angular momentum operator along the X direction. One can also replace $|X\rangle$, $|Y\rangle$, $|Z\rangle$ by a triplet of internal states selected among a more complex level scheme [17]. Our scheme will apply provided each pair of states can be coupled by a resonant two-photon Raman transition with a negligible spontaneous emission rate [18].

We assume that $|X\rangle$, $|Y\rangle$, $|Z\rangle$ are the eigenstates of the atomic Hamiltonian in the absence of atom-laser coupling. We suppose that these three states are nondegenerate and nonequally spaced, and their energies are such that $E_X < E_Y < E_Z$, with $E_Z - E_Y \neq E_Y - E_X$. For alkali atoms this situation can be reached by illuminating the atomic sample with microwaves close to the hyperfine resonance (see Supplemental Material [19]). We denote by z the (1, 1, 1) direction of the X, Y, Z trihedron, and assume that the center-of-mass motion of the atoms along the direction z is frozen. Therefore, we consider, in the following, only the atomic motion in the perpendicular xy plane [see Fig. 1(a)].

The atoms are irradiated with laser beams propagating in the xy plane along three directions making an angle of $2\pi/3$ with each other. The three wave vectors are $\boldsymbol{k}_1 = k/2(\sqrt{3}\boldsymbol{u}_x + \boldsymbol{u}_y)$, $\boldsymbol{k}_2 = k/2(-\sqrt{3}\boldsymbol{u}_x + \boldsymbol{u}_y)$, and $\boldsymbol{k}_3 = -k\boldsymbol{u}_y$, where $\{\boldsymbol{u}_x, \boldsymbol{u}_y\}$ is an orthogonal unit basis of the xy plane.

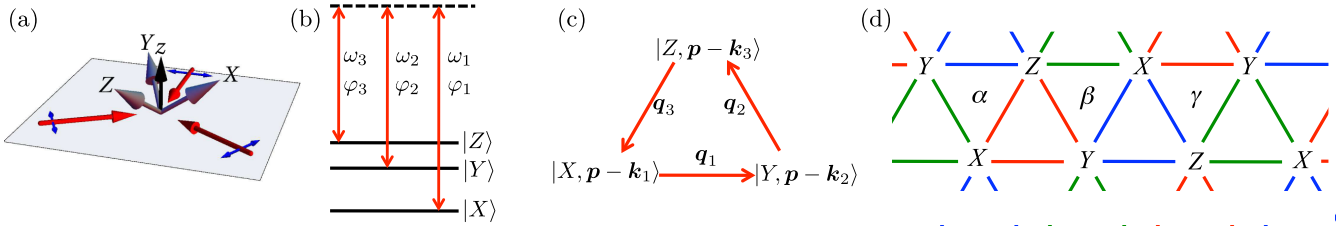

FIG. 1 (color online). (a) Atoms with a ground state with angular momentum $J_g = 1$ are irradiated by three laser running waves propagating in the xy plane, whose wave vectors $\boldsymbol{k}_i$, $i = 1, 2, 3$ make an angle of $2\pi/3$ with each other. (b) Triplet of light frequencies ω_i ensuring that the three possible Raman transitions are resonantly driven. (c) Graphic representation of three internal + momentum eigenstates, which are resonantly coupled by the laser beams whose frequencies are shown in (b). (d) Infinite array of internal + momentum eigenstates that are resonantly coupled when three triplets of frequencies ω_i (red), ω_i' (green), ω_i'' (blue) are simultaneously applied. (See Table I for full details, without requiring color information.)

Here k stands for the typical wave number of the laser beams. We choose the frequency components in each laser beam so that an atom can undergo resonant Raman transitions between the three internal states, by absorbing a photon in one wave and emitting a photon in a stimulated manner in another wave. The momentum change in such a transition is $\pm\boldsymbol{q}_i$, where $\boldsymbol{q}_i = \boldsymbol{k}_i - \boldsymbol{k}_{i+1}$. Here, we set $\boldsymbol{k}_4 \equiv \boldsymbol{k}_1$ and take $\hbar = 1$.

Suppose first that each beam i consists only of a monochromatic plane wave with frequency ω_i and phase φ_i, and that the values of ω_i are chosen such that the three Raman conditions are fulfilled: $\omega_1 - \omega_2 = E_Y - E_X$, $\omega_2 - \omega_3 = E_Z - E_Y$, [and thus, $\omega_1 - \omega_3 = E_Z - E_X$, see Fig. 1(b)]. For each momentum $\boldsymbol{p}$ there is coherent coupling of three states $\{|X, \boldsymbol{p} - \boldsymbol{k}_1\rangle, |Y, \boldsymbol{p} - \boldsymbol{k}_2\rangle, |Z, \boldsymbol{p} - \boldsymbol{k}_3\rangle\}$ forming an equilateral triangle in momentum space [Fig. 1(c)]. This coupling can be written (see Supplemental Material [19])

$$\hat{V} = -\Omega(|Y\rangle\langle X|e^{i(\boldsymbol{q}_1\cdot\boldsymbol{r}+\varphi_1-\varphi_2)} + |Z\rangle\langle Y|e^{i(\boldsymbol{q}_2\cdot\boldsymbol{r}+\varphi_2-\varphi_3)} + |X\rangle\langle Z|e^{i(\boldsymbol{q}_3\cdot\boldsymbol{r}+\varphi_3-\varphi_1)}) + \text{H.c.}, \quad (1)$$

where H.c. stands for Hermitian conjugate. The amplitude and sign of Ω can be adjusted by tuning the laser intensities and their detuning from the atomic resonance. That all three Raman transitions in Eq. (1) have the same amplitude is ensured by (i) taking the same intensity for each laser beam, and (ii) choosing in-plane linear polarizations. A similar ring-coupling scheme was used in Ref. [20] to implement the Peierls substitution in a 1D optical lattice. However, in Ref. [20], only two laser Raman transitions were used and the ring was closed using radio frequency transitions, which is not appropriate for our purpose.

With only one triplet of laser frequencies as in Fig. 1(b), we do not produce the desired infinite periodic lattice for the atomic motion in momentum space [15]. However, this goal can be reached by adding, inside the beams i, two other triplets of frequency components ω_i' and ω_i'', $i = 1, 2, 3$. Here, the roles are circularly exchanged with respect to the first triplet ω_i: the ω_i' (respectively, ω_i'') are such that $\omega_2' - \omega_3' = E_Y - E_X$ and $\omega_3' - \omega_1' = E_Z - E_Y$ (respectively, $\omega_3'' - \omega_1'' = E_Y - E_X$ and $\omega_1'' - \omega_2'' = E_Z - E_Y$). We suppose that the differences between the average frequencies $\bar{\omega}$, $\bar{\omega}'$, $\bar{\omega}''$ of the triplets are much larger than the splittings $E_\alpha - E_\beta$. Raman processes involving absorption from a frequency triplet and emission in another triplet, thus, play a negligible role.

With the three frequency triplets acting simultaneously on an atom, the family of states that are coupled to a given initial state can be represented by the infinite lattice in momentum space shown in Fig. 1(d). Since there are three possible Raman transitions and three possible pairs of beams to induce a given transition, the atom-laser coupling $\hat{V}$ generalizing (1) is now characterized by nine matrix elements. These elements depend on the nine phases $\varphi_i^{(',")}$ and are summarized in Table I, from which it is straightforward to construct the coupling $\hat{V}$.

In order to characterize the possible nontrivial topology associated with the lattice in momentum space, we now evaluate the total phase gained by an atom when it undergoes a series of Raman transitions $X \to Y \to Z \to X$ that cause it to travel around one of the triangles of Fig. 1(d). The resulting phase is different for upwards pointing triangles [such as the one of Fig. 1(c)] and downwards pointing ones [triangles labelled α, β, γ in Fig. 1(d)]. For an upwards pointing triangle, the phase is always zero. Indeed, moving around its sides involves absorption

TABLE I. Phases of the Raman coupling matrix elements. Each line corresponds to a given momentum kick $\boldsymbol{q}_i = \boldsymbol{k}_i - \boldsymbol{k}_{i+1}$, and each column to a given pair of internal atomic states. This 3×3 array can be understood as a determinant: each of the six terms appearing in the calculation of this determinant corresponds to one of the six types of triangles in Fig. 1(d). The terms with a positive (negative) sign in the determinant calculation are for the upwards (downwards) pointing triangles.

	$X \to Y$	$Y \to Z$	$Z \to X$
$\boldsymbol{q}_1$	$e^{i(\varphi_1 - \varphi_2)}$	$e^{i(\varphi_1'' - \varphi_2'')}$	$e^{i(\varphi_1' - \varphi_2')}$
$\boldsymbol{q}_2$	$e^{i(\varphi_2' - \varphi_3')}$	$e^{i(\varphi_2 - \varphi_3)}$	$e^{i(\varphi_2'' - \varphi_3'')}$
$\boldsymbol{q}_3$	$e^{i(\varphi_3'' - \varphi_1'')}$	$e^{i(\varphi_3' - \varphi_1')}$	$e^{i(\varphi_3 - \varphi_1)}$

and stimulated emission of photons whose frequencies belong to the same triplet, e.g., ω_i for Fig. 1(c). Therefore each laser phase $\varphi_i^{(\prime,\prime\prime)}$ enters both with a + and a − sign in the total accumulated phase, leading to a null result.

Downwards pointing triangles, on the other hand, correspond to a nontrivial phase. Consider for example the clockwise oriented path around the sides of triangle α in Fig. 1(d): (i) the $X \rightarrow Y$ transition is accompanied by a change of atomic momentum $\boldsymbol{q}_2$, and a phase change $\varphi_2' - \varphi_3'$ (see Table I); (ii) the $Y \rightarrow Z$ transition is along $\boldsymbol{q}_1$, with the phase change $\varphi_1'' - \varphi_2''$; (iii) the $Z \rightarrow X$ transition is along $\boldsymbol{q}_3$, with the phase change $\varphi_3 - \varphi_1$. As a result, the phase accumulated around triangle α is

$$\Phi_\alpha = \varphi_1'' - \varphi_1 + \varphi_2' - \varphi_2'' + \varphi_3 - \varphi_3'. \tag{2}$$

We can, similarly, calculate the phases $\Phi_{\beta,\gamma}$ for the two other downwards pointing triangles. Although $\Phi_\alpha + \Phi_\beta + \Phi_\gamma = 0$, we can identify configurations such that each phase takes a nontrivial value. For example the choice $\varphi_1 = 2\pi/3$, $\varphi_3 = -2\pi/3$, and all other $\varphi_i^{(\prime,\prime\prime)} = 0$ yields

$$\Phi_\alpha = \Phi_\beta = \Phi_\gamma = 2\pi/3 \mod 2\pi. \tag{3}$$

From now on, we will stick to this choice, together with the assumption that $\Omega > 0$, which is obtained for an alkali-metal atom by tuning the lasers between the D_1 and D_2 resonance lines.

In a practical implementation, all frequency components can be derived from the same monochromatic laser source. The frequencies $\omega_i^{(\prime,\prime\prime)}$ and phases $\varphi_i^{(\prime,\prime\prime)}$ of beam i can be set by a single acousto-optic modulator driven by a programmable function generator, and injected in the same optical fibre. There is no need to control the path lengths of the three optical beams with interferometric precision since their contributions cancel in the phases $\Phi_{\alpha,\beta,\gamma}$. For example, if the path length of beam 1 increases by ℓ, both phases φ_1 and φ_1'' entering in (2) increase by $k\ell$, and Φ_α is unchanged. Physically this cancellation originates from the fact that, on this circuit, the atom both absorbs and emits a photon in each of the beams.

The OFL formed in this way has a reciprocal lattice spanned by the basis vectors $\boldsymbol{G}_1 = 3\boldsymbol{q}_1$ and $\boldsymbol{G}_2 = \boldsymbol{q}_2$. The real space lattice vectors are $\boldsymbol{a}_1 = [2\pi/(3\sqrt{3}q)](\sqrt{3}\boldsymbol{u}_x + \boldsymbol{u}_y)$ and $\boldsymbol{a}_2 = [4\pi/(\sqrt{3}q)]\boldsymbol{u}_y$, where $q = |\boldsymbol{q}_i| = \sqrt{3}k$. This geometry is equivalent to that of the three-state triangular OFL of Ref. [15]. However, the phases in the reciprocal space tight binding model differ: here we have phases 0 and $2\pi/3$ for the upwards and downwards pointing triangles, as opposed to $\pi/3$ for each [15]. Nevertheless, the properties of the OFLs are very similar: in each real-space unit cell the lowest energy dressed state experiences $N_\phi = 1$ flux quantum; the resulting low-energy bands are analogous to Landau levels. In particular, the lowest band has Chern number 1, and very narrow energy width, W, over a broad range of lattice depths Ω. Here, we focus on the case $\Omega = 3E_R$ [where $E_R \equiv q^2/(2m)$ is the recoil energy for atomic mass m] close to which this bandwidth has a (local) minimum of $W \simeq 0.015E_R$ [21]. In view of this very small bandwidth, the system is highly susceptible to the formation of strongly correlated phases even for relatively weak interactions.

We have used exact diagonalization to study the ground states of interacting bosons occupying the lowest energy band of the OFL for $\Omega = 3E_R$. (We neglect the population of higher bands, since the gap to the next band is very large, $\Delta \simeq 46W$.) We consider the bosons to interact via spin-independent contact interactions, which is a good approximation for ^{87}Rb. We write the two-dimensional coupling constant as $g_{2D} = \frac{\hbar^2}{m}\tilde{g}$, where $\tilde{g}$ is dimensionless. For atoms with 3D scattering length a_s restricted to 2D by a harmonic confinement of oscillator length a_0, and neglecting (sub)band mixing, this is $\tilde{g} = \sqrt{8\pi}a_s/a_0$ [22]. We study a finite system in a periodic geometry, with sides $\boldsymbol{L}_1 = N_1\boldsymbol{a}_1$ and $\boldsymbol{L}_2 = N_2\boldsymbol{a}_2$, where $N_{1,2}$ are integers. The total flux is then $N_\phi = N_1N_2$, so for N particles the Landau level filling factor is $\nu \equiv N/N_\phi$. We determine the low-energy spectrum of the many-body system at each (total) crystal momentum using standard Lanczos methods.

For very weak interactions, $\tilde{g} \ll 1$, the bosons form a condensate in the minima of the band dispersion. However, we find that even for moderate interactions $\tilde{g} \gtrsim 0.2$ this (compressible) condensed phase is replaced by strongly correlated (incompressible) FQH states at filling factors $\nu = 1/2$, $2/3$, $3/4$, and 1. Here, we focus on the FQH states at $\nu = 1/2$ and 1. (Results for $\nu = 2/3$, $3/4$ are described in the Supplemental Material [19].)

Evidence for the appearance of incompressible phases is found by calculating the discontinuity in the chemical potential $\Delta\mu$ for the ground state: the difference between the chemical potential for adding a particle and that for removing a particle. A nonzero and positive $\Delta\mu$ indicates that the system is incompressible. To minimize finite-size effects, we define [23] $\Delta\mu \equiv N[E_{N+1}/(N+1) + E_{N-1}/(N-1) - 2E_N/N]$, where E_N is the ground state energy for N particles.

In Fig. 2, we plot the dependence of $\Delta\mu$ on interaction strength $\tilde{g}$. For $\nu = 1/2$ there is an onset of incompressibility for $\tilde{g} \gtrsim 0.2$, and for $\nu = 1$, incompressibility appears for $\tilde{g} \gtrsim 0.4$. In the thermodynamic limit, $N \rightarrow \infty$, the transitions from compressible $\Delta\mu = 0$ to incompressible $\Delta\mu > 0$ should be sharp, and can even be discontinuous for first-order transitions, but are rounded in Fig. 2 by finite-size effects.

To explore the nature of the incompressible phases, it is instructive to study their excitation spectra. Each incompressible phase evolves continuously as $\tilde{g}$ increases; we focus on the limit $\tilde{g} \rightarrow \infty$ which is representative of this phase. We still restrict particles to the lowest 2D band, so

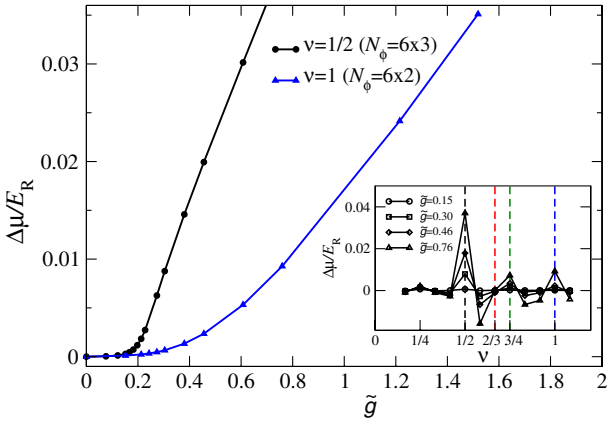

FIG. 2 (color online). Incompressibility, as measured by the discontinuity in the chemical potential $\Delta\mu$ defined in the text, as a function of interaction strength $\tilde{g}$ at several filling factors: $\nu = 1/2$ (for $N = 9$ bosons in a system of size $N_\phi = N_1 N_2 = 6 \times 3$, circles); and $\nu = 1$ ($N = 12$ in $N_\phi = 6 \times 2$, triangles). The inset shows $\Delta\mu$ as a function of filling factor for a series of interaction strengths $\tilde{g}$.

this limit is equivalent to reducing the bandwidth to zero. The spectra, Fig. 3, show all the expected properties of the bosonic Laughlin ($\nu = 1/2$) and Moore-Read ($\nu = 1$) states. On this periodic geometry, these topologically ordered incompressible phases have ground state degeneracies (of 2 and 3, respectively) in the thermodynamic limit, separated by an energy gap from the remaining excitations. Even for the finite systems of Fig. 3, these ground state degeneracies appear clearly. Results on other system sizes and geometries (not shown) confirm that these near degeneracies are robust topological features, not imposed by symmetries.

While suggestive, the ground state degeneracy alone is insufficient to establish the nature of these phases. To achieve this, we show that they are equivalent to the phases that appear for the continuum lowest Landau level (LLL), which are known to be the Laughlin state ($\nu = 1/2$) and the Moore-Read state ($\nu = 1$) [1]. We establish this

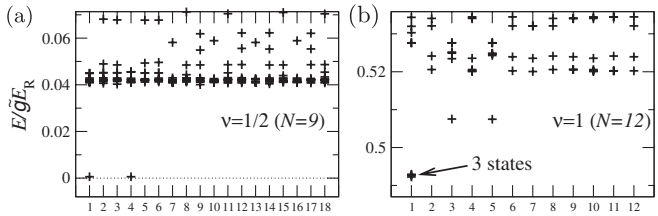

FIG. 3. Low-energy spectra for the OFL with $\Omega/E_R = 3$ in the strong-interaction limit $\tilde{g} \to \infty$ at filling factors (a) $\nu = 1/2$ ($N = 9$ bosons in $N_\phi = N_1 N_2 = 6 \times 3$) and (b) $\nu = 1$ ($N = 12$ bosons in $N_1 N_2 = 6 \times 2$). The crystal momentum $\boldsymbol{k} \equiv \alpha_1 \boldsymbol{G}_1/N_1 + \alpha_2 \boldsymbol{G}_2/N_2$ is labelled by the index, $i = 1 + \alpha_1 + N_1 \alpha_2$ for $\alpha_1 = 0, \ldots, N_1 - 1$ and $\alpha_2 = 0, N_2 - 1$. The quasi-degenerate ground states have the expected multiplicities and crystal momenta for the Laughlin state ($\nu = 1/2$), and the Moore-Read state ($\nu = 1$).

equivalence by studying the evolution of the many-body spectrum for a series of Bloch wave functions that interpolate between those of the lowest band of the OFL and those of the LLL. To do so, we consider a fictitious atom with $N_s = 12$ internal states, and represent the LLL by the $N_s = 12$ triangular OFL of Ref. [15], the lowest band of which has properties that are indistinguishable from those of the LLL for suitable coupling $\Omega' \simeq 10 E_R$ [24]. We place nine additional internal states at the midpoints of the bonds of Fig. 1(d), coupled to each other and to the original states X, Y, Z by bonds of strength Ω' and with $\pi/12$ flux through each new triangular plaquette [25]. Choosing $(\Omega, \Omega') = (3(1 - \lambda), 10\lambda) E_R$ and varying λ leads to smooth interpolation of the lowest energy band and the many-body spectrum, from those of the present model ($\lambda = 0$) to those of the LLL ($\lambda = 1$). In all cases ($\nu = 1/2, 2/3, 3/4, 1$), the energy gap remains open, independent of boundary conditions, and showing no evidence of closing in the thermodynamic limit. This adiabatic continuity establishes the equivalence of these topological phases [26,27], guaranteeing that all topological characteristics are the same. Indeed, under this interpolation, we find very little change in the spectra, showing that this OFL is a very close representation of the LLL. For example, for the LLL, the $\nu = 1/2$ state has zero interaction energy, as the two-body correlation function vanishes exactly at zero range. Here, the $\nu = 1/2$ state in the OFL has $E_N/N \simeq 7 \times 10^{-5} \tilde{g} E_R$ [see Fig. 3(a)] showing that the zero-range two-body correlation function nearly vanishes.

To summarize, we have proposed a robust atom-laser configuration that can lead to FQH states of bosons in a well-accessible range of parameters. The minimal interaction strength $\tilde{g} \approx 0.2$ for obtaining FQH states corresponds to a 2D confinement frequency of $\gtrsim 7$ kHz for Rb, which is readily achieved in an optical lattice. A clear signal of the formation of strongly correlated phases would be the appearance of density plateaus in *in situ* images of the gas, arising from incompressibility $\Delta\mu > 0$. For the Laughlin state, we find from Fig. 2 $\Delta\mu \approx 0.02 E_R$ for $\tilde{g} = 0.4$, that is, 10 nK for ^{87}Rb, setting the temperature scale at which these features can be observed.

This work was supported by the Royal Society of London, EPSRC Grant No. EP/J017639/1 (NRC), IFRAF and ANR (Grant No. AGAFON). We acknowledge useful discussions with J. Beugnon, L. Corman, C. Cohen-Tannoudji, F. Gerbier, G. Möller, and S. Nascimbène.

[1] N. R. Cooper, Adv. Phys. **57**, 539 (2008).
[2] M. Lewenstein, A. Sanpera, V. Ahufinger, B. Damski, A. Sen(De), and U. Sen, Adv. Phys. **56**, 243 (2007).
[3] A. S. Sørensen, E. Demler, and M. D. Lukin, Phys. Rev. Lett. **94**, 086803 (2005).
[4] G. Möller and N. R. Cooper, Phys. Rev. Lett. **103**, 105303 (2009).

[5] L. Mazza, M. Rizzi, M. Lewenstein, and J. I. Cirac, Phys. Rev. A **82**, 043629 (2010).
[6] T. Neupert, L. Santos, C. Chamon, and C. Mudry, Phys. Rev. Lett. **106**, 236804 (2011).
[7] D. N. Sheng, Z.-C. Gu, K. Sun, and L. Sheng, Nat. Commun. **2**, 389 (2011).
[8] Y.-F. Wang, Z.-C. Gu, C.-D. Gong, and D. N. Sheng, Phys. Rev. Lett. **107**, 146803 (2011).
[9] N. Regnault and B. A. Bernevig, Phys. Rev. X **1**, 021014 (2011).
[10] L. Hormozi, G. Möller, and S. H. Simon, Phys. Rev. Lett. **108**, 256809 (2012).
[11] Y.-F. Wang, H. Yao, Z.-C. Gu, C.-D. Gong, and D. N. Sheng, Phys. Rev. Lett. **108**, 126805 (2012).
[12] A. Sterdyniak, N. Regnault, and G. Möller, Phys. Rev. B **86**, 165314 (2012).
[13] N. R. Cooper, Phys. Rev. Lett. **106**, 175301 (2011).
[14] N. R. Cooper and J. Dalibard, Europhys. Lett. **95**, 66 004 (2011).
[15] N. R. Cooper and R. Moessner, Phys. Rev. Lett. **109**, 215302 (2012).
[16] G. Moore and N. Read, Nucl. Phys. **B360**, 362 (1991).
[17] D. L. Campbell, G. Juzeliūnas, and I. B. Spielman, Phys. Rev. A **84**, 025602 (2011).
[18] The three states $|X\rangle$, $|Y\rangle$, $|Z\rangle$ can also stand for different motional states, such as the first three vibrational states along the strongly confined direction z. However, in this case, the hypothesis of a single, state-independent interaction strength should be relaxed.
[19] See Supplemental Material at http://link.aps.org/supplemental/10.1103/PhysRevLett.110.185301 for the derivation of the atom-laser coupling for our OFL configuration and additional numerical results for the many-body spectra.
[20] K. Jiménez-Garcia, L. J. LeBlanc, R. A. Williams, M. C. Beeler, A. R. Perry, and I. B. Spielman, Phys. Rev. Lett. **108**, 225303 (2012).
[21] The bandwidth increases by less than $10^{-3}E_{\mathrm{R}}$ within the range $\Omega/E_{\mathrm{R}} = 2$–$4$.
[22] Z. Hadzibabic and J. Dalibard, Riv. Nuovo Cimento **34**, 389 (2011).
[23] N. R. Cooper, N. K. Wilkin, and J. M. F. Gunn, Phys. Rev. Lett. **87**, 120405 (2001).
[24] Deviations from the continuum Landau level fall exponentially with N_s [15], and are negligible for $N_s = 12$.
[25] This new model has net flux $\pi/3$ through each triangle of Fig. 1(d). In connecting the new (Ω') bonds to those (Ω) of the original model (with fluxes of 0 and $2\pi/3$ through upwards and downwards pointing triangles), we assign flux $\pi/3$ through the loop formed by the two sets of bonds spanning each link $\boldsymbol{q}_3$.
[26] T. Scaffidi and G. Möller, Phys. Rev. Lett. **109**, 246805 (2012).
[27] Y.-H. Wu, J. K. Jain, and K. Sun, Phys. Rev. B **86**, 165129 (2012).